Geology

Incipient faulting near Lake Pillsbury, California, and the role of accessory faults in plate boundary evolution

Amanda M. Thomas, Roland Bürgmann and Douglas S. Dreger

Email alerting services	click www.gsapubs.org/cgi/alerts to receive free e-mail alerts when new articles cite this article
Subscribe	click www.gsapubs.org/subscriptions/ to subscribe to Geology
Permission request	click http://www.geosociety.org/pubs/copyrt.htm#gsa to contact GSA

Notes

THE
GEOLOGICAL
SOCIETY
OF AMERICA

Incipient faulting near Lake Pillsbury, California, and the role of accessory faults in plate boundary evolution

Amanda M. Thomas, Roland Bürgmann, and Douglas S. Dreger
Berkeley Seismological Laboratory, Department of Earth and Planetary Science, University of California–Berkeley, 307 McCone Hall, Berkeley, California 94720, USA

ABSTRACT

We compare the spatiotemporal progression, geometry, and earthquake source characteristics of a zone of anomalous swarm seismicity between the Maacama and Bartlett Springs faults (California, United States) within the northern San Andreas fault system to both laboratory studies of fracture initiation and structural field observations of fault formation. The similarities between laboratory and field studies of incipient faulting and the earthquake swarms suggest that the seismic lineament on which the swarms occur is a fault in an early stage of development. Kinematic descriptions of faulting and models of fault system development suggest that the ability of existing faults to accommodate deformation across plate boundaries is governed by the length scales over which they accommodate stress. Many of the characteristics of juvenile fault zones, such as segmentation, geometric complexity, and the depth extent of faulting, act to reduce this length scale; this requires the reactivation of existing faults or production of accessory faults to accommodate deformation across the plate boundary.

INTRODUCTION

The 1200-km-long San Andreas fault system contains a continuous record of 25 m.y. of plate boundary evolution between the central section of the San Andreas fault in southern California (United States) and the Mendocino triple junction, where formation, reactivation, or growth of faults must occur to accommodate plate boundary evolution (Kelsey and Carver, 1988). Deformation between the Pacific and North American plates near the Mendocino triple junction is accommodated on the San Andreas, Maacama, and Bartlett Springs faults (Kelsey and Carver, 1988; Furlong and Schwartz, 2004). Prior to 2000, the region between the Maacama and Bartlett Springs faults (shown in Fig. 1) was a seismically quiescent area. Local geology includes the Middle Mountain synformal block (KJgv in Fig. 1), which largely consists of a fault-bounded section of folded Cretaceous and early Tertiary interbedded sandstones, siltstones, and shales of the Great Valley Group, oriented N30°W and plunging ~30°NW (R. McLaughlin, 2012, personal commun.; Huffman, 1969). This block is juxtaposed with undifferentiated, weakly metamorphosed Franciscan lithologies to the southwest and northeast, and local ophiolitic rocks to the east and west, along the Pomo and Bucknell Creek faults, respectively (Ohlin et al., 2010).

ANOMALOUS SEISMIC ACTIVITY

In March 2000 an earthquake swarm, lasting ~6 mo and culminating in an M_w 4.4 earthquake, occurred along the eastern edge of the Middle Mountain block (Fig. 1; Hayes et al., 2006). The swarm began with a month-long period of intense microseismicity that preceded the 17 May 2000 shallow M_w 4.4 event. During the next 3 mo, microseismicity propagated to the southeast from 3 to 8 km depth at a rate of 70 m/day and eventually a second M_w 4.0 earthquake occurred (Fig. 2, profile AF). Elevated earthquake activity occurred in the area for the next 6 yr, and in mid-2006 another intense swarm occurred that propagated bilaterally at a rate of 9 m/day and included an M_w 4.8 earthquake. We refer to the 2000 and 2006–2007 swarms as S1 and S2, respectively. Precise earthquake locations (Waldhauser and Schaff, 2008) from both swarms illuminate discontinuous, geometrically complex structure. In the south (Fig. 2, profile D)
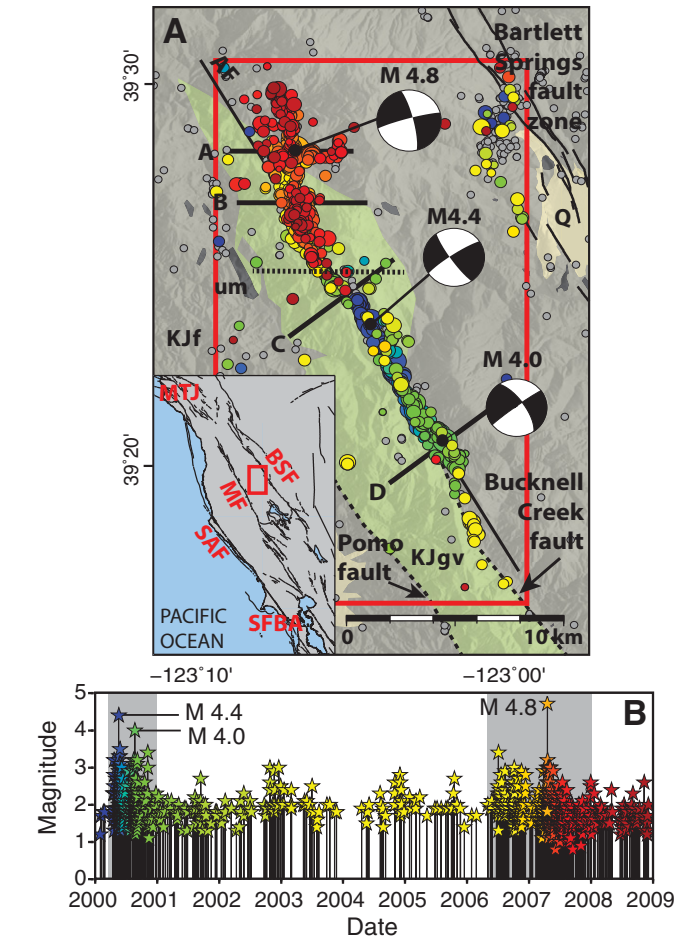

Figure 1. A: Geologic map of Middle Mountain–Lake Pillsbury region (California, United States; modified from Langenheim et al., 2007). Bucknell Creek and Pomo faults are assumed to be coincident with eastern and western contacts of Middle Mountain block (KJgv) south of profile C. Inset map shows regional tectonic map; study area is defined in red. Relocated earthquake hypocenters from 2000 to 2009 are color coded by date shown in B and sizes are scaled relative to earthquake magnitude. Double couple moment tensor solutions are shown for three largest earthquakes, M_w 4.8, M_w 4.4, and M_w 4.0. Lines labeled A–D indicate locations of cross-section profiles shown in Figure 2. Horizontal dotted line marks divide between northern and southern events relevant to Figure 3. KJf—undifferentiated Franciscan complex, KJgv—Great Valley sequence, um—ultramafics and serpentinite, Q—Quaternary fill. Inset map: MTJ—Mendocino triple junction, BSF—Bartlett Springs fault, MF—Maacama fault, SAF—San Andreas fault, SFBA—San Francisco Bay area. Fault trace data were provided by J. Lienkaemper (Lienkaemper and McNutt, 2010). B: Magnitude and date of earthquake hypocenters.

some seismicity occurs shallowly at ~2 km; however, the majority of hypocenters are aftershocks of the M_w 4.0 event and cluster between 5 and 8 km depth. Continuing northwest along strike, seismicity shallows and localizes onto a nearly vertical structure extending from 1 to 6 km depth in profile C, near the M_w 4.4 earthquake. Further north, shallow, diffuse
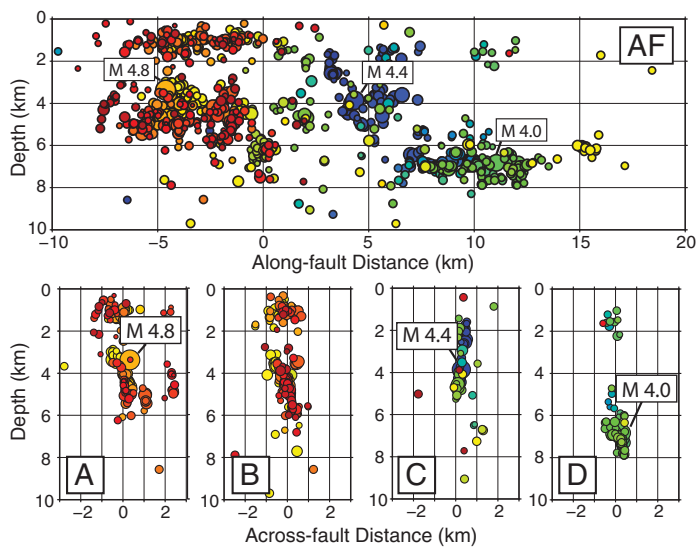
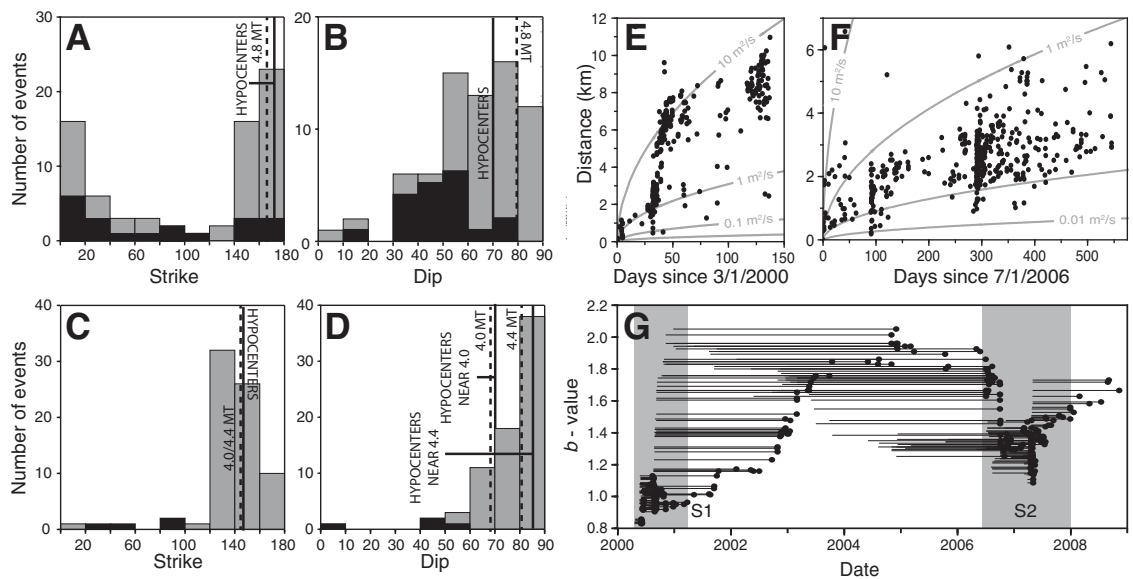Figure 2. Cross sections of seismicity; locations indicated in Figure 1.

seismicity extends between the surface and 3 km depth (Fig. 2, profiles A and B); in this same area deeper events delineate an approximately north-south–striking plane dipping 70°NE in profile B.

To further constrain lineament geometry we compute focal mechanisms for all events with more than 25 first motion observations and full-waveform moment tensors for the 3 largest events (Hardebeck and Shearer, 2002; Dreger, 2003; Minson and Dreger, 2008). Figure 3 compares moment tensor solutions for the 2000 M_w 4.4, 2000 M_w 4.0, and 2007 M_w 4.8 events, populations of fault plane solutions of nearby earthquakes, and the geometry defined by the earthquake hypocenters. In S1, focal mechanisms and moment tensor solutions indicate that nearly all events are right-lateral strike-slip earthquakes that occur on structures

striking parallel to the Maacama and Bartlett Springs faults (Fig. 3C). Many of these events occur on vertically dipping fault planes; however, some seismicity occurs on more shallowly dipping structures (Fig. 3D). In S2, mechanisms are predominantly right-lateral strike-slip and normal faulting events (Figs. 3A and 3B). The hypocenter locations indicate that faulting below 3 km depth occurs, on average, along an ~N10°W trending plane that dips to the northeast (Figs. 3A and 3B). We also calculate the average b-value, or the slope of the earthquake frequency-magnitude distribution, as a function of time for a moving window of 50 events (Fig. 3G; Fig. DR5 in the GSA Data Repository[1]). The b-value reflects the relative proportion of large- to small-magnitude events, with small b-values indicating a larger number of intermediate and large magnitude events and vice versa. The b-values for crustal earthquakes are generally close to 1; on average, S1, the time period between the S1 and S2 swarms, and S2 have b-values of 0.93, 1.99, and 1.40, respectively.

While similar in strike, the moment tensor solution for this event has a dip of 79°, steeper than the majority of earthquakes in the northern swarm (Fig. 3B). In a survey of northern California focal mechanisms, Castillo and Ellsworth (1993) found that right-lateral transform motion between the North American and Pacific plates commonly occurs on structures dipping between 50° and 75°; they suggested that these structures may have formed as reverse faults in the forearc of the Cascadia subduction zone and will eventually evolve to the vertical strike-slip geometry of the major faults in the San Andreas fault system. The seismicity of the swarms may reflect the transition between these two styles of deformation, as many events in S2 occur on a structure dipping 70°NE ~10 km north of the more mature, vertically dipping southern section of the seismically defined fault structure (Fig. 2, profiles B and D). We also note that locations of some earthquakes in S1 align with surficial features, such as a small ridge-top saddle near High Peak, straight stream reaches, and a contact mapped as the Bucknell Creek fault; this may be indicative of faulting at depth (Huffman, 1969; McLaren et al., 2007). We find no morphological evidence of faulting near the northern events in S1 and all events in S2.

Figure 3. Comparison of geometries derived from moment tensor solutions, first motion focal mechanisms, and earthquake hypocenters for seismicity in north (top row, n = 74) and south (bottom row, n = 72). Because mechanisms of shallow seismicity can be highly variable, we limit depth range for north and south event populations to between 3 and 5 km and >3 km, respectively. A–D: Histograms of strike and dip of focal mechanisms compared to fault plane geometries derived from moment tensor solutions of $M_w \geq 4$ events (dashed lines) and geometry delineated by hypocenters (solid lines). Only nodal plane with strike closest to that of lineament was considered. Parts of histogram shown in gray represent fault plane geometries of strike-slip earthquakes; those shown in black are dip-slip events. E: Space-time migration plots for all events in S1. Gray curves are parabolic envelopes for diffusivities ranging from 0.01 to 10 m²/s. F: Space-time migration plots for all events in S2. G: b-values as function of time for moving windows of 50 events. Horizontal lines indicate window duration (longer durations correspond to lower seismicity rates). Because each window contains 50 events, each estimated b-value has uncertainty of ±0.4.

COMPARISON TO INCIPIENT FAULTING IN THE LABORATORY AND IN THE FIELD

Earthquake swarms are commonly linked to volcanic activity, pore pressure diffusion, and aseismic slip (Weaver and Hill, 1978; Hayes et al., 2006; Roland and McGuire, 2009; Chen et al., 2012; Malagnini et al., 2012). One previous study suggests that S1 was induced by a lower crustal dike intrusion, on the basis of nearby seismic reflectors thought to represent lower crustal melt (Hayes et al., 2006). This interpretation is inconsistent with both the orientation of seismicity relative to the maximum principal stress direction (Provost and Houston, 2003) and the existence of shallow seismicity, as a dike intrusion in the lower crust would result in compressive stress in the upper crust, which should inhibit shallow seismicity (Hayes et al., 2006). Swarms thought to result from pore pressure diffusion often have parabolic spatiotemporal migration patterns (e.g., Chen et al., 2012; Malagnini et al., 2012). Figures 3E and 3F show space-time plots for swarms S1 and S2, respectively, and the expected space-time migration seismicity driven by a fluid pressure source in a homogeneous, isotropic medium (diffusivities ranging from 0.01 to 10 m²/s). We note that S1 and S2 are not well fit by these parabolic envelopes, as seismicity often occurs before or lags behind the expected arrival of the front. Fluids may still play a role, however, as considering multiple sources and different diffusivities can result in more complicated migration patterns. Migration rates in the two swarms are orders of magnitude slower than the 0.1–1 km/h slip front velocities observed during aseismic slip events (Roland and McGuire, 2009). Chen et al. (2012) found that many migrating swarms with propagation speeds well below those typically associated with aseismic slip were better fit by linear (versus parabolic) migration, suggesting that these swarms may have been caused by aseismic slip slower than previously reported. Thus, we also cannot rule out the hypothesis that aseismic slip may have been involved. Independent of the specific mechanism, many characteristics of S1 and S2, such as the diversity of focal mechanisms, complex geometry, and changes in the b-value, have also been observed during field and laboratory studies of nascent faulting. Because the seismic lineament is located in a young section of the San Andreas fault system, we suggest that S1 and S2 may be related to incipient fault development.

Structural complexity has been documented extensively in field studies of the initial stages of shear zone development (Martel et al., 1988), and arises for two reasons. First, faults take advantage of preexisting weaknesses, which typically have poor connectivity, and are neither coplanar nor optimally oriented (Crider and Peacock, 2004). Second, to form a throughgoing fault while still exploiting these weaknesses, secondary fractures are generated in response to the stress fields surrounding en echelon cracks (Martel et al., 1988; Crider and Peacock, 2004). Similarly, the seismic lineament is structurally segmented with abrupt changes in geometry in the south and north. The colocation of S1 and the Bucknell Creek fault in the south, and of S2 with relict-dipping structures in the north (Fig. 2, profile B), suggests it may be exploiting preexisting structure as it propagates northward. Such preexisting zones of weakness localize deformation, facilitating the development of new faults with more mechanically favorable orientations. Secondary extensional faulting also occurs, as evidenced by the events with normal mechanisms (Figs. 3A and 3B; Fig. DR4) that have strikes coincident with the approximately north-south direction of the maximum compressive stress (Provost and Houston, 2003).

Swarms of small seismic events, known as acoustic emissions, are observed in laboratory studies of rock fracture (Lockner et al., 1991). Seismicity in S1 and S2 is similar to acoustic emissions observed in laboratory studies of rock fracture in three ways. First, the locations of acoustic emissions evolve from diffuse to localized as fractures nucleate and grow, making acoustic emissions good for diagnosis of strain localization in the different stages of fracture development (Satoh et al., 1990; Lockner et al., 1991). While the deep seismicity in S2 concentrates on a zone of preexisting weakness, the shallow hypocenters are distributed in an ~4-km-wide zone, qualitatively consistent with the precursory localization of acoustic emissions prior to fracture. Second, many researchers report acoustic emission radiation patterns indicative of both shear and tensile cracking during laboratory fracture formation, similar to the strike-slip and normal events in S1 and, particularly, S2 (Satoh et al., 1990; Lei et al., 2000) (Figs. 3A–3D; Fig. DR4). Third, Lockner et al. (1991) reported b-values that decreased drastically, from 2.3 to 1.2, during laboratory fault nucleation and increased to 1.8 following fracture. The temporal variation in b-value prior to and during S2 (Fig. 3G) is nearly identical to that observed in the laboratory.

ROLE OF ACCESSORY FAULTS IN PLATE BOUNDARY EVOLUTION

If the seismic activity near Lake Pillsbury represents a fault in the incipient stages of development, we can gain insight into fault system evolution by asking why additional, accessory faults are needed to accommodate deformation, given that both the Maacama and Bartlett Springs faults are nearby. In kinematic descriptions of faulting, the length scales over which a particular fault can accommodate stress are related to fault geometry, slip, and area. Young faults like the Maacama and Bartlett Springs are often segmented, not optimally oriented, and are structurally complex; this limits the length scale over which those faults can accommodate stress. In young fault systems, accessory faults, such as the seismic lineament illuminated by S1 and S2, form to aid in accommodating stress and may later be abandoned when the major faults become mature enough to relieve stress across the plate boundary (Fig. 4).
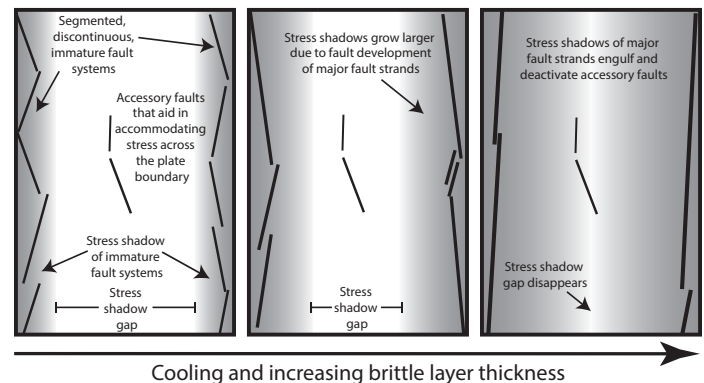

Figure 4. Schematic diagram (map view) of conceptual fault system development model. Time increases from left to right.

The depth extent of faulting may also govern whether accessory faults are needed to accommodate deformation. This idea is supported by models of the fault system evolution that show that fault spacing depends on the depth of faulting and the thickness of the elastic layer in which it occurs (i.e., thinner layers produce tighter fault spacing) (Roy and Royden, 2000). A variety of geophysical data indicates that thermal weakening of the deep crust occurs over a broad region in northern California (Beaudoin et al., 1996; Lachenbruch and Sass, 1980; Griscom and Jachens, 1989). This thermal weakening is thought to be due to the presence of a slab window that propagates in the wake of the Mendocino triple junction and currently extends from 20 km north of Lake Pillsbury south to Clear Lake (Griscom and Jachens, 1989; Castillo and Ellsworth, 1993; Beaudoin et al., 1996). The presence of the slab window has likely thinned the brittle, load-bearing upper crust. This influence is reflected in the depth distribution of seismicity (Castillo and Ellsworth, 1993) and, perhaps, in the surface distribution of faults, as a thinning brittle upper crust should decrease fault spacing and additional accessory faults may be needed to accommodate regional deformation.

CONCLUSIONS

The similarity between the spatiotemporal evolution of S1 and S2 and laboratory and field studies of fault formation shows that the swarms are related to incipient faulting in one of the youngest sections of the San Andreas fault system. We also suggest that in some cases earthquake swarms, such as those near Lake Pillsbury and Reno, Nevada (Bell et al., 2012), are diagnostic of fault initiation and early development. The need to accommodate deformation between the Bartlett Springs and Maacama faults is due to the geometric complexity, segmentation of the major faults in the young northern San Andreas fault system, and thermal weakening of the brittle upper crust. While this provides a mechanism for development of new faults, the specific location of accessory faults, such as the youthful fault zone illuminated by recent swarm seismicity, is also dictated by pre-existing weakness (e.g., fabrics related to subduction), which concentrates strain in areas where faults may eventually nucleate and develop.

REFERENCES CITED

Beaudoin, B.C., Godfrey, N.J., Klemperer, S.L., Lendl, C., Trehu, A.M., Henstock, T.J., Levander, A., Hole, J.E., Meltzer, A.S., Luetgert, J.H., and Mooney, W.D., 1996, Transition from slab to slabless: Results from the 1993 Mendocino triple junction seismic experiment: Geology, v. 24, p. 195–199, doi:10.1130/0091-7613(1996)024<0195:TFSTSR>2.3.CO;2.

Bell, J.W., Amelung, F., and Henry, C.D., 2012, InSAR analysis of the 2008 Reno-Mogul earthquake swarm: Evidence for westward migration of Walker Lane style dextral faulting: Geophysical Research Letters, v. 39, doi:10.1029/2012GL052795.

Castillo, D.A., and Ellsworth, W.L., 1993, Seismotectonics of the San Andreas fault system between Point Arena and Cape Mendocino in northern California: Implication for the development and evolution of a young transform: Journal of Geophysical Research, v. 98, p. 6543–6560, doi:10.1029/92JB02866.

Chen, X., Shearer, P.M., and Abercrombie, R.E., 2012, Spatial migration of earthquakes within seismic clusters in southern California: Evidence for fluid diffusion: Journal of Geophysical Research, v. 117, B04301, doi:10.1029/2011JB008973.

Crider, J.G., and Peacock, D.C.P., 2004, Initiation of brittle faults in the upper crust: A review of field observations: Journal of Structural Geology, v. 26, p. 691–707, doi:10.1016/j.jsg.2003.07.007.

Dreger, D.S., 2003, TDMT_INV: Time Domain Seismic Moment Tensor INVersion: International Handbook of Earthquake and Engineering Seismology, v. 81B, p. 1627.

Furlong, K.P., and Schwartz, S.Y., 2004, Influence of the Mendocino triple junction on the tectonics of coastal California: Annual Review of Earth and Planetary Sciences, v. 32, p. 403–433, doi:10.1146/annurev.earth.32.101802.120252.

Griscom, A., and Jachens, R.C., 1989, Tectonic history of the north portion of the San Andreas fault system, California, inferred from gravity and magnetic anomalies: Journal of Geophysical Research, v. 94, p. 3089–3099, doi:10.1029/JB094iB03p03089.

Hardebeck, J.L., and Shearer, P.M., 2002, A new method for determining first-motion focal mechanisms: Seismological Society of America Bulletin, v. 92, p. 2264–2276, doi:10.1785/0120010200.

Hayes, G.P., Johnson, C.B., and Furlong, K.P., 2006, Evidence for melt injection in the crust of northern California?: Earth and Planetary Science Letters, v. 248, p. 638–649, doi:10.1016/j.epsl.2006.05.008.

Huffman, M.E., 1969, Engineering geology of Garrett Tunnel and Potter Valley conveyance system: State of California Department of Water Resources Memorandum Report.

Kelsey, H.M., and Carver, G.A., 1988, Late Neogene and Quaternary tectonics associated with northward growth of the San Andreas transform fault, northern California: Journal of Geophysical Research, v. 93, p. 4797–4819, doi:10.1029/JB093iB05p04797.

Lachenbruch, A.H., and Sass, J.H., 1980, Heat flow and energetics of the San Andreas fault zone: Journal of Geophysical Research, v. 85, p. 6185–6222, doi:10.1029/JB085iB11p06185.

Langenheim, V.E., Jachens, R.C., Morin, R.L., and McCabe, C.A., 2007, Preliminary gravity and magnetic data of the Lake Pillsbury region, Northern Coast Ranges, California: U.S. Geological Survey Open-File Report 2007-1368, 24 p., http://pubs.usgs.gov/of/2007/1368/.

Lei, X., Kusunose, K., Rao, M.V.M.S., Nishizawa, O., and Satoh, T., 2000, Quasi-static fault growth and cracking in homogeneous brittle rock under triaxial compression using acoustic emission monitoring: Journal of Geophysical Research, v. 105, no. B3, p. 6127–6139, doi:10.1029/1999JB900385.

Lienkaemper, J.J., and McNutt, M.K., 2010, Recently active traces of the Bartlett Springs fault, California: A digital database: U.S. Geological Survey Data Series 541, 13 p., http://pubs.usgs.gov/ds/541/.

Lockner, D.A., Byerlee, J.D., Kuksenko, V., Ponomarev, A., and Sidorin, A., 1991, Quasi-static fault growth and shear fracture energy in granite: Nature, v. 350, p. 39–42, doi:10.1038/350039a0.

Malagnini, L., Lucente, F.P., De Gori, P., Akinci, A., and Munafo, I., 2012, Control of pore fluid pressure diffusion on fault failure mode: Insights from the 2009 L'Aquila seismic sequence: Journal of Geophysical Research, v. 117, B05302, doi:10.1029/2011JB008911.

Martel, S.J., Pollard, D.D., and Segall, P., 1988, Development of simple strike-slip-fault zones, Mount Abbot Quadrangle, Sierra Nevada, California: Geological Society of America Bulletin, v. 100, p. 1451–1465, doi:10.1130/0016-7606(1988)100<1451:DOSSSF>2.3.CO;2.

McLaren, M.K., Wooddell, K.E., Page, W.D., van der Elst, N., Stanton, M.A., and Walter, S.R., 2007, The McCreary Glade earthquake sequence: Possible reactivation of ancient structures near Lake Pillsbury, Northern Coast Ranges, Mendocino County, California: Eos (Transactions, American Geophysical Union), v. 88, fall meeting supplement, abs. S21A–0245.

Minson, S.E., and Dreger, D.S., 2008, Stable inversions for complete moment tensors: Geophysical Journal International, v. 174, p. 585–592, doi:10.1111/j.1365-246X.2008.03797.x.

Ohlin, H.N., McLaughlin, R.J., Moring, B.C., and Sawyer, T.L., 2010, Geologic map of the Bartlett Springs fault zone in the vicinity of Lake Pillsbury and adjacent areas of Mendocino, Lake, and Glenn Counties, California: U.S. Geological Survey Open-File Report 2010-1301, scale 1:30,000, http://pubs.usgs.gov/sim/3125/.

Provost, A., and Houston, H., 2003, Stress orientations in northern and central California: Evidence for the evolution of frictional strength along the San Andreas plate boundary system: Journal of Geophysical Research, v. 108, no. B3, doi:10.1029/2001JB001123.

Roland, E., and McGuire, J.J., 2009, Earthquake swarms on transform faults: Geophysical Journal International, v. 178, p. 1677–1690, doi:10.1111/j.1365-246X.2009.04214.x.

Roy, M., and Royden, L.H., 2000, Crustal rheology and faulting at strike-slip plate boundaries. 1: An analytic model: Journal of Geophysical Research, v. 105, p. 5583–5598, doi:10.1029/1999JB900339.

Satoh, T., Nishizawa, O., and Kusunose, K., 1990, Fault development in Oshima granite under triaxial compression inferred from hypocenter distribution and focal mechanism of acoustic emission: Tohoku Geophysical Journal: Science Reports of the Tohoku University, v. 33, p. 241–250.

Waldhauser, F., and Schaff, D.P., 2008, Large-scale relocation of two decades of northern California seismicity using cross-correlation and double-difference methods: Journal of Geophysical Research, v. 113, B08311, doi:10.1029/2007JB005479.

Weaver, C.S., and Hill, D.P., 1978, Earthquake swarms and local crustal spreading along major strike-slip faults in California: Pure and Applied Geophysics, v. 117, p. 51–64, doi:10.1007/BF00879733.